

Structure of polystyrene latex particles determined by electron microscopy

A. E. Chalykh,^a V. K. Gerasimov,^a U. V. Nikulova,^{a*} A. A. Ezhova,^b and I. A. Gritskova^b

^aA. N. Frumkin Institute of Physical Chemistry and Electrochemistry, Russian Academy of Sciences, Building 4, 31 Leninsky prosp., 119072 Moscow, Russian Federation.

Fax: +7 (495) 952 5308. E-mail: ulianan@rambler.ru

^bMIREA — Russian Technological University,

86 prosp. Vernadskogo, 119571 Moscow, Russian Federation.

E-mail: rector@mirea.ru

The structures of individual polystyrene microspheres obtained in the presence of organosilicon surfactants were studied by transmission electron microscopy. The density of the macromolecule distribution over the cross section of particles was determined. The synthesized latex particles have a core–shell structure.

Key words: dispersion and colloidal systems, supramolecular structure, latex particles, organosilicon surfactants.

Modern analytical transmission electron microscopy (TEM) is one of the most informative methods for studying structural morphological characteristics of materials of diverse nature.^{1–3} The TEM method is based on a quantitative analysis of results of scattering of the monochromatic electron beam upon its passing through an object, including individual nanoparticles, macromolecules, and micelles of biological or synthetic origin.^{4,5} Modern computer software provides fixation of the image and, hence, new (digital) possibilities of its processing and analysis.^{6,7}

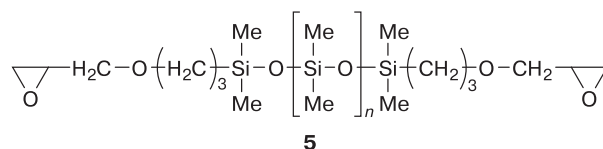
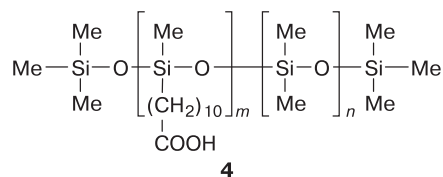
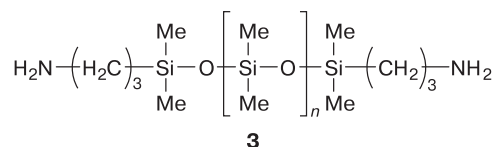
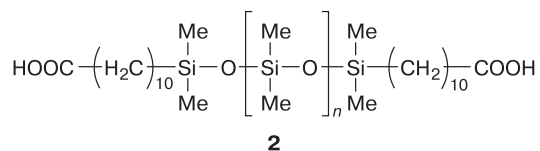
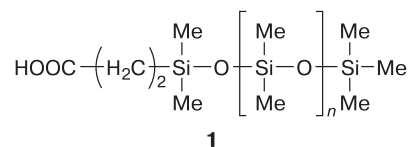
The purpose of the present work is to obtain an information about the structural morphological characteristics of polystyrene microspheres, which were synthesized by heterophase polymerization in the presence of organosilicon oligomers containing carbon- and aminofunctional groups as stabilizers.

The data on the use of water-insoluble surfactants (Surf) as stabilizers of polymer suspensions have first appeared in the works,^{8–10} where the authors showed that the heterophase polymerization of styrene in the presence of oligodimethylsiloxane with carboxydecyl, aminopropyl, glycidoxypropyl, or oligoethylene oxide terminal groups afforded polymer spherical particles with a diameter of 0.4–0.9 μm and a narrow size distribution. The polymer suspensions were stable at the surfactant concentrations much lower than those observed in the presence of usually applied water-soluble hydrocarbon surfactants.¹¹

Experimental

Objects of the study were water-insoluble carboxy- and aminofunctional organosilicon oligomers **1–5** of the linear

structure with different arrangements and different concentrations of the carbofunctional substituents in the siloxane chain (Table 1).



Molecular weights of organosilicon surfactants and polystyrene (PS) were determined by gel permeation chromatography.

Table 1. Characteristics of the initial organosilicon substances

Compound	M_w /g mol ⁻¹	M_w/M_n	ρ /g cm ⁻³
2-(Carboxyethyl)- ω -(trimethylsiloxy)- polydimethylsiloxane (1), $n = 8$	249	1.9	1.00
α,ω -Bis(10-carboxydecyl)- oligodimethylsiloxane (2), $n = 30$	2750	2.0	0.97
α,ω -Bis(3-aminopropyl)- oligodimethylsiloxane (3), $n = 30$	2480	1.8	0.99
α,ω -Bis(trimethylsiloxy)- oligodimethylmethyl- (10-carboxydecyl)sil- oxane (4), $m = 14, n = 32$	4750	1.8	0.98
α,ω -Bis(3-glycidoxypropyl)- polydimethylsiloxane (5), $n = 30$	2600	1.9	0.98

The colloidal chemical properties of the organosilicon substances were described earlier.¹²

Styrene polymerization was carried out at a constant temperature of 80±0.5 °C, the volume ratio of the phases surfactant solution in styrene to water equal to 1 : 9, 1 : 6, or 1 : 4; and the potassium persulfate as an initiator 1 wt.% (based on the monomer). The surfactant concentration was varied from 0.15 to 1.0 wt.% (based on the monomer). The characteristics of polystyrene suspensions obtained in the presence of the organosilicon surfactants of various structure are presented in Table 2.

The structural morphological characteristics of PS latex particles (microspheres) were studied by scanning and transmission electron microscopy. In both cases, a dilute aqueous dispersion of PS particles was deposited on the carbon support and dried at ~20 °C in desiccators with a lowered moisture content (<30%). A gold nanolayer was deposited on the particle surface by thermal sputtering and then the samples were studied with a JSM U3 scanning electron microscope (Japan) at an accelerating voltage of 15 keV and direct electron microscopic amplification from ×1000 to ×10 000.

Table 2. Characteristics of polystyrene suspensions synthesized in the presence of the organosilicon surfactants of various structure*

Surfactant	[Surf] (%)	$d^{**}/\mu\text{m}$	$M_w \cdot 10^{-5}/\text{g mol}^{-1}$
1	1.0	0.43	6.51
2	1.0	0.46	4.23
3	1.0	0.4, 1.8	3.52
4	1.0	0.68	4.45

* Coagulum was absent from all samples.

** Diameter of particles of the polymer suspension according to the dynamic light scattering data.

The PS particles were not additionally treated before studying with an EM-120 transmission electron microscope (Netherlands). The morphology of the particles was examined at an accelerating voltage of 60 keV and direct electron microscopic amplification from ×10 000 to ×50 000. Individual spherical PS particles with a diameter of 300–600 nm, which is substantially shorter than the path length of an electron in a material of unity density, were chosen.¹³

The concentration of carboxyl and aminopropyl groups on the surface of the PS particles was determined by X-ray photoelectron spectroscopy. The photoelectron spectra of the samples were detected on an ESCALAB MK2 electron spectrometer (VG SCIENTIFIC, Great Britain). The radiation of the Mg-K α anode with the photon energy 1253.6 eV was used as a source. The studies were carried out on the samples prepared using the procedure described above for the TEM study.

The particle size distribution was estimated by photon correlation spectroscopy on a Zetasizer Nano ZS laser analyzer of particles (Malvern, Great Britain). The working temperature range was 2–120 °C, the angle of scattered light detection was 173°, a helium–neon laser with the wavelength 633 nm served as a light source, and the power of the light source was 5 mW. The measurements were carried out in an automated mode using a standard procedure.¹⁴

Results and Discussion

The typical images of the PS microspheres synthesized in the presence of compound **2** are presented in Fig. 1. Similar images were obtained for the PS particles synthesized in the presence of compounds **1**, **3**, and **4**. All synthesized particles, regardless of the surfactant concentration, had a distinctly identified spherical shape and a narrow particle size distribution. The D_w/D_n ratio varied in the range 1.11–1.01. The molecular weights of PS obtained in the presence of all studied surfactants are close and equal to $1 \cdot 10^5$ – $6 \cdot 10^5$ g mol⁻¹.

The particle diameter increased from 0.68 to 2.0 μm for compound **4** and from 0.55 to 0.8 μm for compound **2** with an increase in the monomer concentration. The molecular weight of PS somewhat decreased with an increase in the diameter of the particles: from $5.7 \cdot 10^5$ to $2.1 \cdot 10^5$ and from $4.2 \cdot 10^5$ to $2.49 \cdot 10^5$ for compounds **4** and **2**, respectively. The decrease in the molecular weight of the polymer in the particles of a larger diameter is related, most likely, to an increase in the concentration of the radicals in them and to the chain termination reaction.

From 150 to 250 images of individual particles were obtained by the electron microscopic study for each PS sample and processed. It is known in terms of the amplitude contrast that the electron beam passing through the studied amorphous substance and interacting with the substance loses a portion of its energy. A decrease in the beam intensity is associated with the structure, electron density, and atomic properties of the studied substance. This means that a change in the intensity of the electron beam after interaction with the object of the study

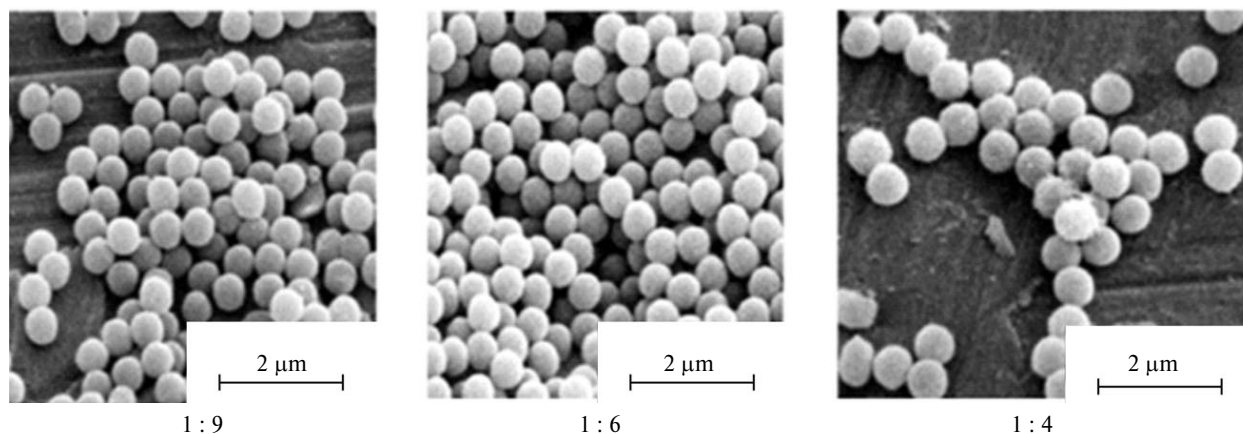


Fig. 1. Images of the PS microspheres obtained in the presence of compound **2** at various ratios of the phases monomer : water. The concentrations of potassium persulfate and surfactant were 1 wt.% (based on the monomer).

bears an information about the internal structure of the object.

An electron microscopic image is traditionally formed on a planar display, and the decrease in the beam intensity appears as a change in the degree of blackening at each point of the image of the object of the study compared to background values. From the geometric point of view, the electron beam is oriented normally to the display on which the image is visualized. Thus, the degree of blackening of each point bears an information about the results of interaction of the electron beam passed along a certain trajectory with the studied object (scattering, absorption, *etc.*).

Since the polymer particles studied are spherical, we may assume that the internal structure of the polymer particles also has the spherical symmetry.

The modern methods of image fixation make it possible to perform numerical analysis of images without restriction only by the external shape of the studied objects. We have previously¹⁵ obtained the equation for the calculation of the radial function of the electron density distribution $\rho(r)$ of spherically symmetrical objects from their function of blackening of the object:

$$\rho(r) = -[\partial F(r)/\partial r]/(2\pi r), \quad (1)$$

where $\rho(r)$ is the density of the spherically symmetrical objects at the distance r from the center of gravity, and $\partial F(r)/\partial r$ is the derivative of the blackening function at the radius.

Transforming the image of the studied object into digits, we obtain the matrix, the rows and columns of which correspond to the coordinates of the point and the values of the elements of the matrix correspond to the degrees of blackening at each point. In turn, the degree of blackening depends on the geometric route of an electron through the studied object and on the number of atoms on which scattering occurs. Thus, the degree of blackening of each point bears a direct information about the composition and density of the studied substance.

Summing the values of degrees of blackening over the rows or columns, we have the unidimensional object (column or row) reflecting the change in the degree of blackening of the spherically symmetrical object, the thickness of which is equal to the distance between two points on the image and the radii are determined by the remoteness of this segment from the center. Thus found dependence of the degree of blackening on the distance from the center of gravity, as a rule, is symmetrical (Fig. 2) and makes it possible to use Eq. (1) for the calculation of the radial function of the density distribution. The radial function of the density distribution determined by the method described above was normed to the density of PS (1.05 g cm^{-3}).

The images and the radial functions of the density distribution obtained by processing these images are shown in Figs 3 and 4. Each of the radial functions of the density distribution is well described by a piecewise linear approximation. We define the region with the radii larger than the radius of the maximal density (I) as the surface layer of the polymer microsphere. Region II of density

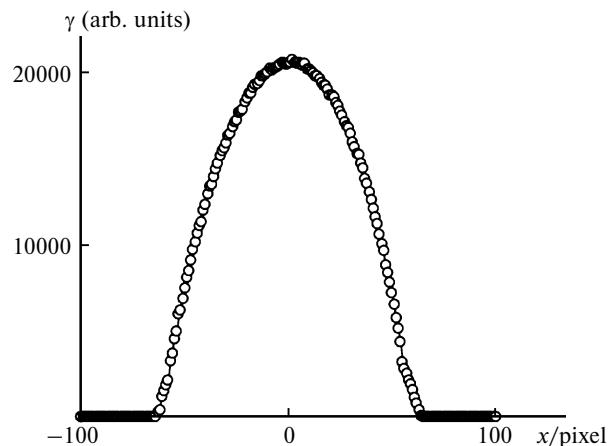


Fig. 2. Degree of blackening (γ) of the image of the PS microsphere obtained in the presence of compound **2**.

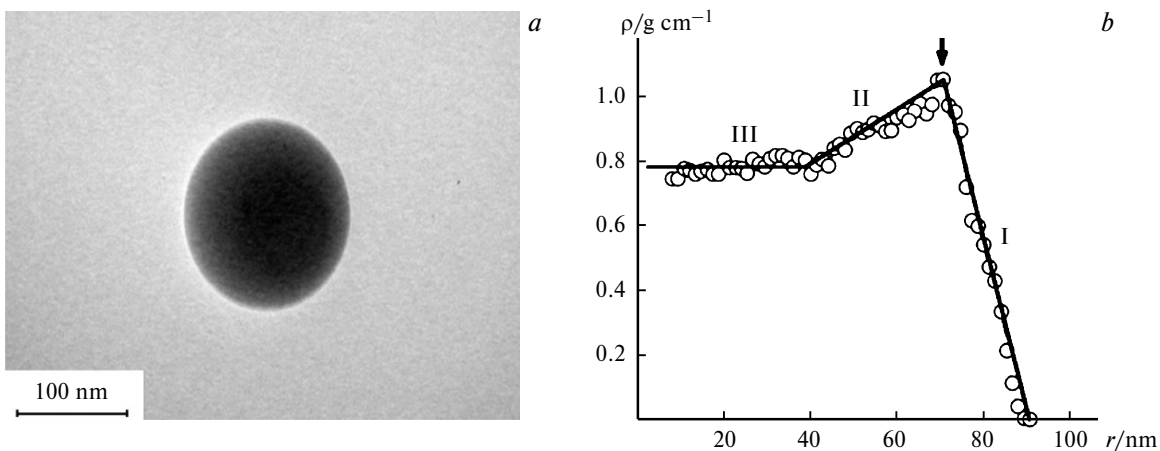


Fig. 3. Image of the polymer microsphere obtained in the presence of compound **2** (a) and the radial function of the density distribution inside the particle (b); I is the surface layer of the particle, II is the near-surface layer of density decreasing, and III is the particle core. Arrow marked the position of the inertia radius.

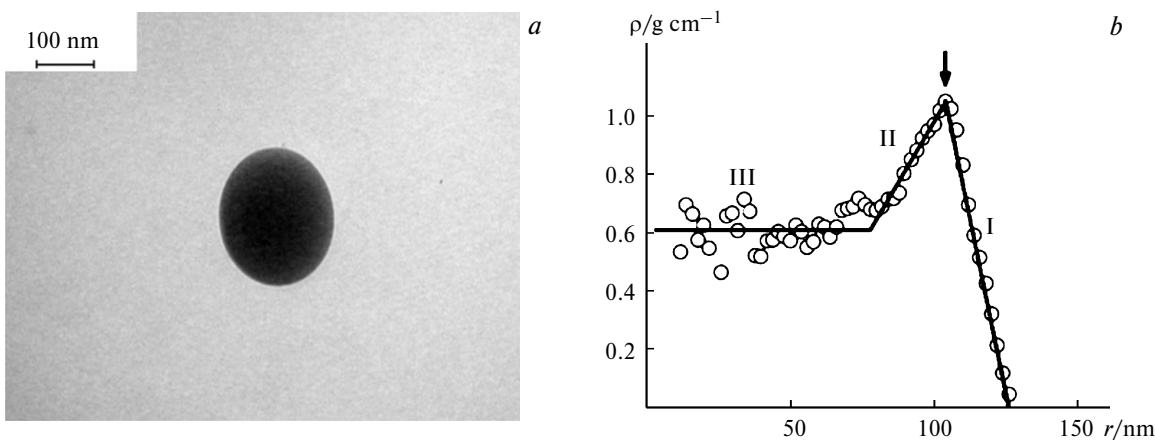


Fig. 4. Image of the polymer microsphere obtained in the presence of compound **3** (a) and the radial function of the density distribution inside the particle (b); I is the surface layer of the particle, II is the near-surface layer of density decreasing, and III is the particle core. Arrow marked the position of the inertia radius.

decreasing on moving along the radius from maximal values to the center of the particle (III) was defined as the "near-surface layer." Their sizes are shown in Table 3 along with the data for polydiphenylmethylsiloxane (**6**) given for comparison.¹⁸

Thus, the synthesized PS particles should be considered as microspheres with a complicated highly organized internal structure of the core–shell type. The structural organization of the latex particle is schematically presented in Fig. 5. When composing the scheme, we took into account the extension of the surface layer and quantitative data on its density, as well as the data of X-ray photoelectron spectroscopy, according to which the ratio of the atomic concentrations C : Si in the surface layer is 4.0, whereas for the surfactant this ratio is 4.9 according to the calculated values.

In the first approximation, we assume that the PS macromolecules are predominantly arranged inside the latex particle, *i.e.*, form the core of the particle. The sur-

face layer of the particle (I) is formed by the surfactant molecules directed by the polar groups toward the aqueous polar disperse medium. It should be emphasized that the radial arrangement of the surfactant chains is idealized to some extent. In fact, an ensemble of surfactant molecules should be considered as statistical, especially in the case of the surfactants with a broad distribution of molecules

Table 3. Average structural characteristics of latex particles

Surfactant	Average size/nm		
	Radius	Surface layer	Near-surface layer of density decreasing
1	52	10.7	17
2	56	12	21
3	62	14	18
5	83	19	26
6	68	17	31

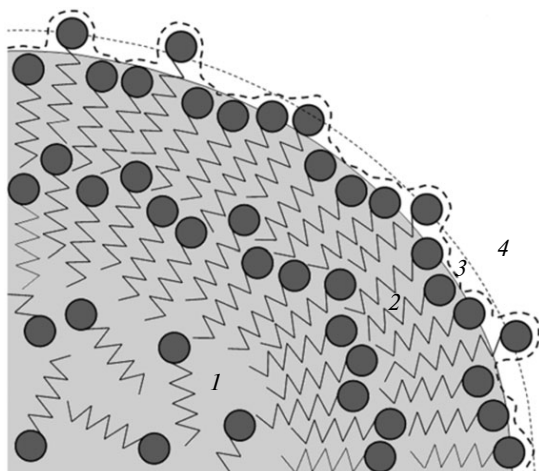


Fig. 5. Scheme of the structural organization of the latex particle: 1, particle core with dissolved surfactant molecules; 2, near-surface layer of the particle; 3, surface layer of the particle characterized by microroughness; and 4, disperse medium.

over molecular weights (see Table 1). Therefore, the external surface of the shell is not also a geometrically rigid surface of the sphere. It is rough in the molecular scale: some polar groups are located above the spherical surface, and other are arranged below the spherical surface.

Note that the thickness of the surface layer of the particles correlates linearly with the thickness of the adsorption layer of surfactants of various structures on the monomer particle (Fig. 6), which was calculated from the results of the independent colloidal chemical measurements.¹² This result suggests an identity of the adsorption protection layer for surfactants of diverse structure used for the synthesis of polymer suspensions. The particle shell can partially be enriched in fragments of PS macromolecules, since for initiation by potassium persulfate the

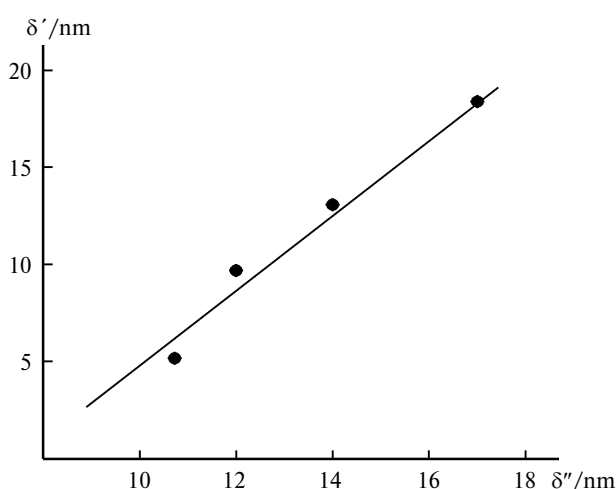


Fig. 6. Relationship between the thickness of the interphase layer of the surfactant on the surface of the monomer particle (δ') and the surface layer of the particle (δ'').

SO_4^{2-} radical anions initiate the polymerization process and fix one end of the polymer chain on the particle surface due to the polarity of the terminal sulfo group.^{16,17}

The radial functions of the density distribution of the polymer particles averaged within one experimental series, which were normed to the position of the density maximum, form a single array of points and they are much smoother (Fig. 7). It can be assumed that this effect indicates the identical mechanism of structure formation for particles of the polymer suspensions obtained in the presence of all studied organosilicon surfactants.

The maximal density of the packing of the PS particles is concentrated in the near-surface layer of the shell, where the highest concentrations and degrees of ordering of the conformational arrangement of the surfactant molecules are likely observed. When the figurative point moves deep into the particle, the packing density of the segments of the polymer molecules decreases and the concentration of surfactant molecules dissolved in the phase of the polymer—monomer particle simultaneously decreases. This structure of the shell also containing macromolecular fragments provides its high stability, which results in the stabilization of the geometric sizes of the polymer microspheres. According to the dynamic light scattering data, this stabilization effect takes place already at low conversions of the monomer (Fig. 8), when the particle core represents PS swollen by the monomer. Thus, no change in the constant volume occurs upon the polymerization of the monomer, and this results in the formation of particles with an excessive free volume in the core and, as a consequence, with a decreased density of the polymer, which is distinctly identified in the images and curves of the density distribution (see Figs 3 and 4).

The concepts on the mechanism of structure formation of polymer particles should be supplemented by the data on phase transitions that occur in PS—styrene—Surf solutions

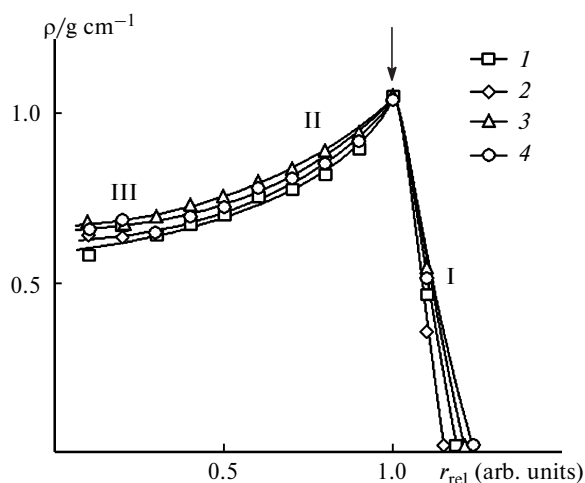


Fig. 7. Radial functions of the density distribution of the microspheres obtained in the presence of compounds 1 (1), 2 (2), 3 (3), and 4 (4), which were normed to the position of the particle maximum. The designations are the same as in Figs 3 and 4.

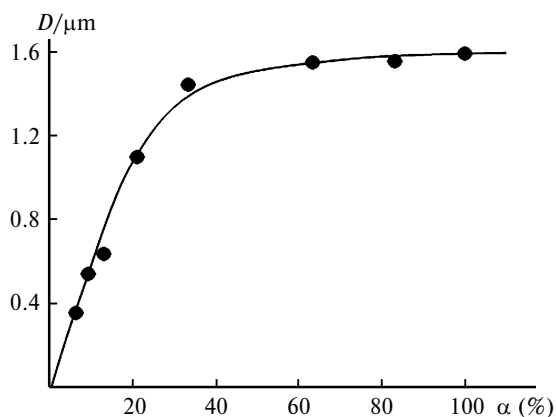


Fig. 8. Dependence of the diameter of PS microspheres (D) on the conversion of the monomer (α).

during the polymerization of the monomer. We have previously^{18,19} determined the amorphous separation diagrams in the indicated system for PS of low molecular weights. The phase decomposition of the solution with a change in the molecular weight of the polymer was experimentally studied and an assumption was advanced that the solubility of the surfactant decreases in the core of the polymer particles during styrene polymerization, which results in the migration of surfactant molecules to the phase of the shell.

To conclude, the obtained results allowed us to propose the following hypothesis about the formation of polymer—monomer particles and interphase layers on their surface. The hypothesis is based on the data^{20,21} on studying the Langmuir films of the organosilicon surfactants. The amount of Surf I the interphase layer of the polymer—monomer particle increases in the course of polymerization because of their enforced diffusion from the volume to the particle surface, since the organosilicon surfactants are incompatible with the formed polymer. Spiral structures (if assuming their *cis*-isomerization) with the functional groups oriented to the aqueous phase are formed during the displacement of the Surf molecule. The formation of the spirals is accompanied by the stage of displacement of the functional groups to the aqueous phase. At the maximal compression (end of polymerization) the spirals of the organosilicon chains are laminated on each other to form supramolecular structures, which is accompanied by an increase in the interphase layer thickness.

The studies were carried out on the equipment of the Center for Collective Use of the A. N. Frumkin Institute of Physical Chemistry and Electrochemistry of the Russian Academy of Sciences.

This work was financially supported by the Russian Foundation for Basic Research (Project No. 17-03-00197).

References

1. A. S. Vishnevskii, A. E. Chalykh, S. A. Pisarev, V. K. Gerasimov, *Fizikokhim. Poverkhn. Zashch. Mater. [Physico-*

- chemistry of Surface and Material Protection]*, 2017, **53**, 153 (in Russian).
2. *Polymer Blends. Vol. 1. Formulation*, Eds D. R. Paul, C. B. Bucknall, Wiley, New York, 2000.
3. A. E. Chalykh, A. D. Aliev, A. E. Rubtsov, *Elektronno-zondovyi rentgenospektral'nyi analiz v issledovanii polimerov [X-Ray Electron Probe Spectral Analysis in Investigation of Polymers]*, Nauka, Moscow, 1990, 192 pp. (in Russian).
4. R. Henderson, J. M. Baldwin, T. A. Ceska, F. Zemlin, E. Backmann, K. H. Downing, *J. Mol. Biol.*, 1990, **213**, 899.
5. J. Dubochet, A. W. McDowell, *J. Microscopy*, 1981, **124**, 3.
6. A. S. Vishnevskii, A. E. Chalykh, V. K. Gerasimov, O. V. Stoyanov, *Vestn. Kazan. Tekhnol. Un-ta [Bull. Kazan Technol. Univ.]*, 2013, **16**, No. 1, 246 (in Russian).
7. A. S. Vishnevskii, A. E. Chalykh, V. K. Gerasimov, V. V. Matveev, O. V. Stoyanov, *Vestn. Kazan. Tekhnol. Un-ta [Bull. Kazan Technol. Univ.]*, 2017, **20**, No. 6, 15 (in Russian).
8. O. V. Chirikova, I. A. Gritskova, O. I. Shchegolikina, A. A. Zhdanov, *Dokl. Akad. Nauk*, 1994, **334**, 57 [*Dokl. Chem. (Engl. Transl.)*, 1994].
9. I. A. Gritskova, D. I. Shragin, S. M. Levachev, A. A. Ezhova, E. V. Milushkova, V. M. Kopylov, S. A. Gusev, N. I. Prokopov, N. A. Lobanova, *Tonkie Khim. Tekhnol. [Fine Chemical Technologies]*, 2016, **11**, No. 2, 5 (in Russian).
10. I. A. Gritskova, V. S. Papkov, I. G. Krasheninnikova, A. M. Evtushenko, *Vysokomol. Soedin. Ser. A*, 2007, **49**, 389 [*Polym. Sci., Ser. A (Engl. Transl.)*, 2007, **49**].
11. K. Holmberg, B. Jonsson, B. Kronberg, B. Lindman, *Surfactants and Polymers in Aqueous Solution*, John Wiley & Sons, New York, 2002.
12. I. A. Gritskova, A. A. Ezhova, A. E. Chalikh, S. M. Levachev, S. N. Chvalun, *Russ. Chem. Bull.*, 2019, **68**, 132.
13. A. K. Pikaev, *Sovremennaya radiatsionnaya khimiya. Osnovnye polozeniya, eksperimental'naya tekhnika i metody [Modern Radiation Chemistry. The Main Statements, Experimental Technique, and Methods]*, Nauka, Moscow, 1985, 81 pp. (in Russian).
14. *Determination of Particle Size. Photon Correlation Spectroscopy*, ISO TS 24/SC4/WG7 Fourth Draft, 1993.
15. V. K. Gerasimov, A. E. Chalykh, *Vysokomol. Soedin. Ser. B*, 2001, **43**, 2015 [*Polym. Sci., Ser. B (Engl. Transl.)*, 2001, **43**].
16. C. S. Chern, *Prog. Polym. Sci.*, 2006, **31**, 443.
17. I. A. Gritskova, S. V. Zhachenkov, M. S. Tsar'kova, S. M. Levachev, G. A. Simakova, M. Khaddazh, N. I. Prokopov, *Vysokomol. Soedin. Ser. B*, 2011, **53**, 1994 [*Polym. Sci., Ser. B (Engl. Transl.)*, 2011, **53**].
18. A. A. Ezhova, Thesis (Chem.) Cand. Sci., MTU-MIREA, Moscow, 2019, 178 pp. (in Russian).
19. A. A. Poteryaev, Thesis (Chem.) Cand. Sci., Institute of Physical Chemistry and Electrochemistry, Russian Academy of Sciences, Moscow, 2018, 165 pp. (in Russian).
20. A. A. Ezhova, I. A. Gritskova, A. E. Chalykh, S. M. Levachev, D. I. Shragin, S. N. Chvalun, Yu. N. Malakhova, A. M. Muzafarov, *Vysokomol. Soedin. Ser. A*, 2019, **61**, 125 [*Polym. Sci., Ser. A (Engl. Transl.)*, 2019, **61**].
21. I. A. Gritskova, V. G. Lakhtin, D. I. Shragin, A. A. Ezhova, I. B. Sokolskaya, I. N. Krizhanovsky, P. A. Storozhenko, A. M. Muzafarov, *Russ. Chem. Bull.*, 2018, **67**, 1908.

Received February 28, 2019;
in revised form April 29, 2019;
accepted May 20, 2019